J. Fluid Mech. (1982), *vol.* 121, *pp.* 403–424
Printed in Great Britain

Parametric solutions for breaking waves

By M. S. LONGUET-HIGGINS

Department of Applied Mathematics and Theoretical Physics,
University of Cambridge, Silver Street, Cambridge, England,
and Institute of Oceanographic Sciences, Wormley, Surrey

(Received 8 September 1981 and in revised form 15 February 1982)

Time-dependent flows such as occur in breaking surface waves are often most conveniently described in parametric form, with the coordinate z and velocity potential χ each expressed in terms of a third complex variable ω and the time t.

In this paper we discuss some interesting flows given in terms of elementary functions of ω and t. Included are the Stokes 120° corner flow, the 45° rotor or rotating wedge, and a decelerated upwelling flow, with an exactly plane surface.

Lastly it is shown that a class of cubic flows, which are related to the plane upwelling flow just mentioned, has a free surface that corresponds with remarkable accuracy to the forward face of an overturning, or plunging, breaker.

1. Introduction

The phenomenon of *overturning* exhibited by surface gravity waves in both deep and shallow water still lacks a satisfactory mathematical description. Figures 1 and 2 illustrate two salient features of the flow. First, it must be highly time-dependent, with particle accelerations comparable to, or even much larger than, g. Mathematical techniques for dealing with free-surface flows of this kind have been suggested in some recent papers (Longuet-Higgins 1980*a*, *b*, 1981),† particularly in paper I.

The second feature, illustrated more especially by figure 2, is that when the jet impinges on the forward face of the wave the relatively smooth flow becomes sharply discontinuous. Mathematically, the flow can be regarded as a multivalued function. It is as though the colliding particles are attempting to pass onto another sheet of the Riemann surface. This in turn implies at least a simple branch point in the velocity potential, located somewhere in the 'tube' of the breaking wave.

(We are here interested only in describing the flow up to the moment of impact. Afterwards, a different type of description will become necessary, involving perhaps turbulence and entrained flow.)

In conventional descriptions of irrotational flow, the velocity potential χ is usually expressed directly in terms of the complex coordinate z in the plane of motion, with the time t as an additional variable. In papers I and II a more flexible scheme was suggested, in which χ and z were each expressed as analytic functions of a third complex variable ω, and also t. As pointed out in § 2 below, this has the advantage that the simplest kind of zero, where $dz/d\omega$ vanishes at some point $\omega = \omega_0$, say, corresponds to the simplest kind of branch point in the velocity potential χ and its

† To be referred to as I, II and III respectively.

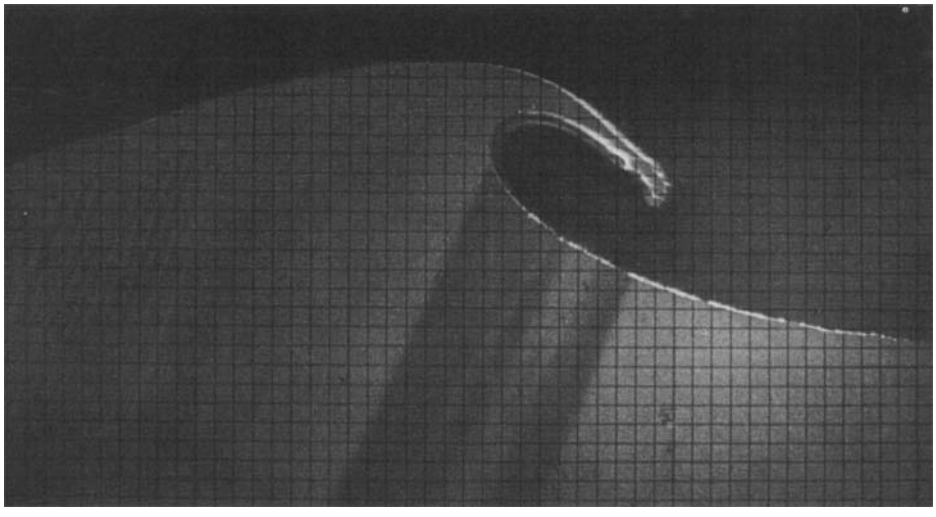

FIGURE 1. Profile of a plunging breaker (from Miller 1957).

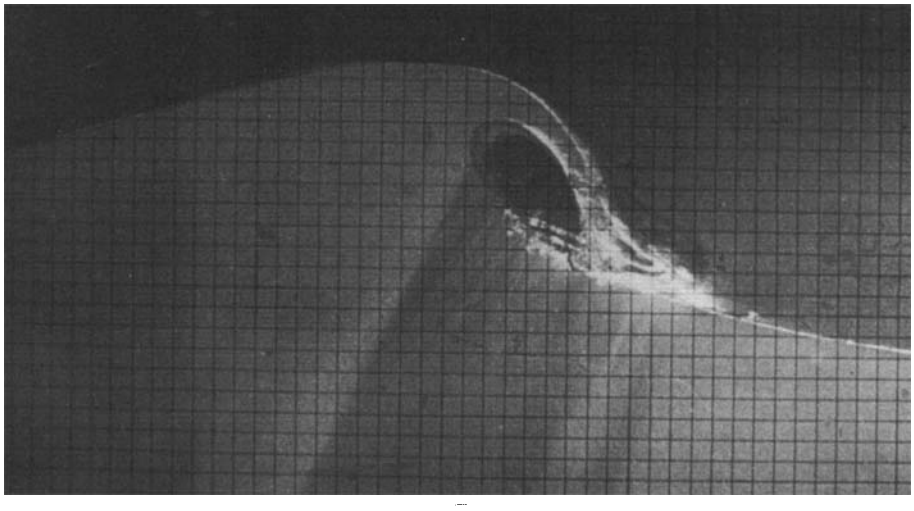

FIGURE 2. Tip of a plunging breaker striking the forward face of the wave (from Miller 1957).

derivatives. Such a parametric description therefore seems possibly very appropriate to our problem.

Some years ago John (1953) suggested a particular type of parametric representation in which the parameter ω was assumed to be Lagrangian, in the sense of being constant following a given particle. This leads to certain simplifications (see I). However, in deriving physical solutions, John's chief preoccupation was to *avoid* the occurrence of zeros in $dz/d\omega$, or at least to ensure that the corresponding singularities were annulled by zeros in the velocity gradient. In our problem, on the other hand, the zeros of $dz/d\omega$ are very much to be desired, provided that they occur fairly close to the domain of the flow, and outside it.

A second feature of John's analysis was to assume the parameter ω to take only *real* values at the free surface. This assumption enables a velocity potential $\chi(\omega, t)$ to be found in the interior, corresponding to a given motion of the free surface. For the general problem, the assumption is probably too restrictive. Nevertheless, our purpose here will be to examine whether certain simple flows that do accord with John's second assumption (namely that ω is real at the free surface) are of any use in describing the overturning of surface waves.

Already some results in this direction have been given in a previous paper (Longuet-Higgins 1976). But all the flows described there were gravity-free, in the sense that the acceleration g did not appear in the solution. The flows were appropriate to a reference frame in free fall, or to the cases where the particle accelerations are large compared with g. As pointed out in § 5 below, gravity-free flows correspond to a certain linear and homogeneous boundary condition for $z(\omega, t)$. To include gravity, we must solve a non-homogeneous equation. But, once a particular integral is found, further solutions of the homogeneous equation may be added as a kind of complementary function.

As a first example we present a simple parametric description of the well-known Stokes corner flow, in which gravity is of course included. An analogous flow is the '45° rotor' discovered in paper II, for which a parametric representation is given in § 7.

We then pass on to discuss an interesting type of gravity flow (§ 8). This can be described as a 'decelerated upwelling', in which the pressure gradient from the surface velocities is exactly balanced by that due to the deceleration. Associated with this is a family of flows given as simple polynomials in ω. Remarkably, it appears that one of the cubic polynomials agrees very closely with the observed profiles of overturning waves.

Further discussion is given in § 14.

2. Parametric representation; branch points

We consider incompressible, irrotational flow in two dimensions, where the velocity potential $\chi = \phi + i\psi$ is in general an analytic function of the position coordinate $z = x + iy$ and of the time t. Instead of expressing χ directly as a function of z and t we assume that χ and z are each analytic functions of a third complex variable ω, and of t. Thus by eliminating ω between χ and z we could if we wished express χ directly as an analytic function of z, except at a singularity.

Consider the flow in the neighbourhood of a branch point. If suffixes are used to denote partial differentiation, with respect to ω or t, then the particle velocity is given by W^*, where

$$W = \chi_\omega / z_\omega \tag{2.1}$$

and an asterisk denotes the conjugate complex quantity. Suppose that z_ω has a simple zero at $\omega = \omega_0$, where $z = z_0$. Then in the neighbourhood of this point we have

$$z - z_0 \sim \tfrac{1}{2}(\omega - \omega_0)^2 z_{\omega\omega}. \tag{2.2}$$

Hence

$$\omega - \omega_0 \propto (z - z_0)^{\frac{1}{2}}, \tag{2.3}$$

and if χ is a regular and analytic function of ω with $\chi_{\omega_0} \neq 0$ then

$$\chi - \chi_0 \sim (\omega - \omega_0)\chi_\omega \propto (z - z_0)^{\frac{1}{2}} \tag{2.4}$$

also. This represents the simplest type of branch-point singularity. The velocity χ_z^* is $O(z-z_0)^{\frac{1}{2}}$ and so less singular than in a source of vortex, where it is $O(z-z_0)^{-1}$.

If, as in § 4, the velocity W^* is finite at $\omega = \omega_0$, as well as the potential χ, then by a similar argument $W - W_0$ is generally $O(z-z_0)^{\frac{1}{2}}$ and $\chi - \chi_0$ is $O(z-z_0)^{\frac{3}{2}}$.

3. Boundary conditions

General expressions for the pressure p and its rate of change Dp/Dt following a particle were given in paper I. Thus if g denotes gravity, and if the x-axis is taken pointing downwards, from Bernoulli's equation we have

$$-2p = (\chi_t - Wz_t) + \text{c.c.} + WW^* - g(z+z^*) - 2f, \tag{3.1}$$

in which f is a function of t only, and 'c.c.' denotes the complex conjugate of the preceding terms. Also

$$-2\frac{Dp}{Dt} = [(\chi_{tt} - Wz_{tt}) + 2K(\chi_{\omega t} - Wz_{\omega t}) + K^2(\chi_{\omega\omega} - Wz_{\omega\omega})] + \text{c.c.} - g(W+W^*) - 2f_t, \tag{3.2}$$

where

$$K = \frac{D\omega}{Dt} = \frac{W^* - z_t}{z_\omega}. \tag{3.3}$$

At a (moving) free surface, the boundary conditions are that

$$p = 0, \quad Dp/Dt = 0. \tag{3.4}$$

In the special case when ω is a Lagrangian coordinate, constant following a particle, then clearly

$$z_t = W^*, \quad K = 0, \tag{3.5}$$

and so (3.2) reduces to

$$-2\frac{Dp}{Dt} = (\chi_{tt} - Wz_{tt}) + \text{c.c.} - g(W+W^*) - 2f. \tag{3.6}$$

Some solutions making use of the equations (3.1) and (3.2) in this general form were given in papers II and III.

4. Method of John

The above equations may be considered as a generalization of the approach of John (1953), who assumed, in addition to the flow being Lagrangian, that the parameter ω was *real* at the free surface. So at the free surface we have both

$$W^* = z_t(\omega) \tag{4.1}$$

and

$$\chi_\omega/z_\omega = W = z_t^*(\omega^*) = z_t^*(\omega) \tag{4.2}$$

since $\omega = \omega^*$. Therefore (at the free surface)

$$\chi_\omega = z_\omega(\omega)\, z_t^*(\omega), \tag{4.3}$$

and a flow satisfying at least the kinematic boundary condition may be found by integrating with respect to ω:

$$\chi = \int^\omega z_\omega(\omega)\, z_t^*(\omega)\, d\omega. \tag{4.4}$$

This is always provided that χ has no singularities, including zeros of z_ω unaccompanied by zeros of W_ω, within the domain of the fluid. On the contrary, branch points *outside* the fluid may be welcome, for reasons given in § 1.

In John's formulation the dynamical boundary condition becomes especially simple for, since ω is Lagrangian at the surface, the particle acceleration there is simply z_{tt}. Hence the pressure gradient is $z_{tt}-g$, which must be normal to the free surface. But, since ω is real, the tangent to the surface is in the direction of z_ω. So we must have

$$z_{tt}-g = irz_\omega, \tag{4.5}$$

where r is some function of ω and t which is real on the boundary.

In the interior of the fluid, however, ω is not necessarily Lagrangian. There, by virtue of (4.4), we have

$$\chi_\omega = z_\omega(\omega)\, z_t^*(\omega) \tag{4.6}$$

(see (4.3)), and so the particle velocity is given by

$$W = (\chi_\omega/z_\omega)^* = z_t(\omega^*), \tag{4.7}$$

not $z_t(\omega)$, as it would be if ω were Lagrangian everywhere. Only at the free surface, where $\omega = \omega^*$, is the velocity given by $z_t(\omega)$.

For this reason we shall need the more general expressions for p and Dp/Dt given by (3.1) and (3.2). Making use of (4.7) these may be rewritten more explicitly as follows. First

$$-2p = (\chi_t+\chi_t^*)+z_t(\omega^*)\, z_t^*(\omega)-g(z+z^*)-2f-[z_t(\omega)\, z_t^*(\omega)+z_t(\omega^*)\, z_t^*(\omega^*)]. \tag{4.8}$$

It will be noted that this is a function of ω, ω^* and t. If $F(\omega, \omega^*, t)$ is any such function, it is clear that

$$\frac{DF}{Dt} \equiv F_t + KF_\omega + K^*F_{\omega^*}, \tag{4.9}$$

where $K = D\omega/Dt$ is given by (3.3). In the present case, since $W^* = z_t(\omega^*)$, we have

$$K = [z_t(\omega^*)-z_t(\omega)]/z_\omega. \tag{4.10}$$

With $F = -2p$ and K given by (4.10), we find in fact that (4.9) reduces to

$$-2\frac{Dp}{Dt} = [(\chi_{tt}-Wz_{tt})+2Kz_\omega z_{tt}^*(\omega)+K^2z_\omega z_{t\omega}^*(\omega)]+\text{c.c.}-g(W+W^*)-2f_t. \tag{4.11}$$

But from (4.6)

$$\chi_{\omega t}-Wz_{\omega t} = z_{tt}^*(\omega)\, z_\omega, \tag{4.12}$$

$$\chi_{\omega\omega}-Wz_{\omega\omega} = z_{t\omega}^*(\omega)\, z_\omega. \tag{4.13}$$

Hence (4.11) is equivalent to (3.2).

Lastly we note that, though the particle acceleration a at the surface, in John's formulation, is simply equal to z_{tt}, in the interior it must be calculated from the more general formula

$$a = \frac{D}{Dt}z_t(\omega^*) = z_{tt}(\omega^*)+K^*z_{t\omega^*}(\omega^*), \tag{4.14}$$

K^* being the conjugate of (4.10).

5. Frames of reference

Given a suitable function $r(\omega, t)$, real when ω is real, the boundary condition

$$z_{tt} - g = irz_\omega \tag{5.1}$$

may be regarded as a non-homogeneous linear differential equation for $z(\omega, t)$. Let $z_0(\omega, t)$ be any solution of (5.1). Then it is clear that $z_0 + z_1(\omega, t)$ is also a solution, provided only that z_1 satisfies the homogeneous equation

$$z_{tt} = irz_\omega \tag{5.2}$$

with the same integrating function r. We may call z_0 a *particular integral* of the equation (5.1). Then z_1, in general form, is the *complementary function*, and $z_0 + z_1$ the complete integral.

Since (5.2) can be derived from (5.1) simply by setting $g = 0$, (5.2) can be regarded also as a gravity-free form of (5.1), and we may think of solutions to (5.2) as *free-fall solutions*, that is solutions to (5.1) but seen in a reference frame moving with downward acceleration g.

Thus, if $z_0(\omega, t)$ is any solution of (5.1), then

$$z_1 = z_0 - \tfrac{1}{2}gt^2 \tag{5.3}$$

is a solution to (5.2), and conversely. It is easy to verify from (4.8) that the pressure $p(\omega, \omega^*, t)$ remains unaltered, apart from an additive function of the time t. The corresponding velocities, however, will differ by the amount gt, which may be important in matching inner flows to an outer flow as $t \to -\infty$.

In other respects the distinction between a solution to (5.1) and (5.2) need not be important, particularly in situations where the particle accelerations are large compared with g, or are highly variable. In § 6 we shall examine a flow which in one reference frame, including gravity, is steady, but in another, free-falling frame is an expanding, self-similar flow.

6. The Stokes corner flow

As a first application consider the familiar flow proposed by Stokes (1880) to describe the limiting form of a progressive wave crest, seen by an observer moving horizontally with the phase speed. Take the origin O at the wave crest and the axis of $\mathscr{R}(z)$ pointing vertically downwards as in figure 3(*a*). (The wave is moving to the right.) A particle on the forward face of the wave travels up the slope with deceleration $\frac{1}{2}g$, the inclination to the vertical being $\frac{1}{3}\pi$ or $\arccos\frac{1}{2}$. If each particle is labelled by the time ω at which it reaches the wave crest, then the position $z(\omega, t)$ of the particle ω at time $t < \omega$ is given by

$$z = \tfrac{1}{4}g\, e^{i\pi/3}(\omega - t)^2. \tag{6.1}$$

(A characteristic of progressive motion is that z is a function of $\omega - t$ only.)

To verify the free-surface condition, note that

$$z_\omega = \tfrac{1}{2}g\, e^{i\pi/3}(\omega - t) \tag{6.2}$$

and

$$z_{tt} - g = \tfrac{1}{2}g(e^{i\pi/3} - 2) = \tfrac{1}{2}\sqrt{3}\, ig\, e^{i\pi/3}, \tag{6.3}$$

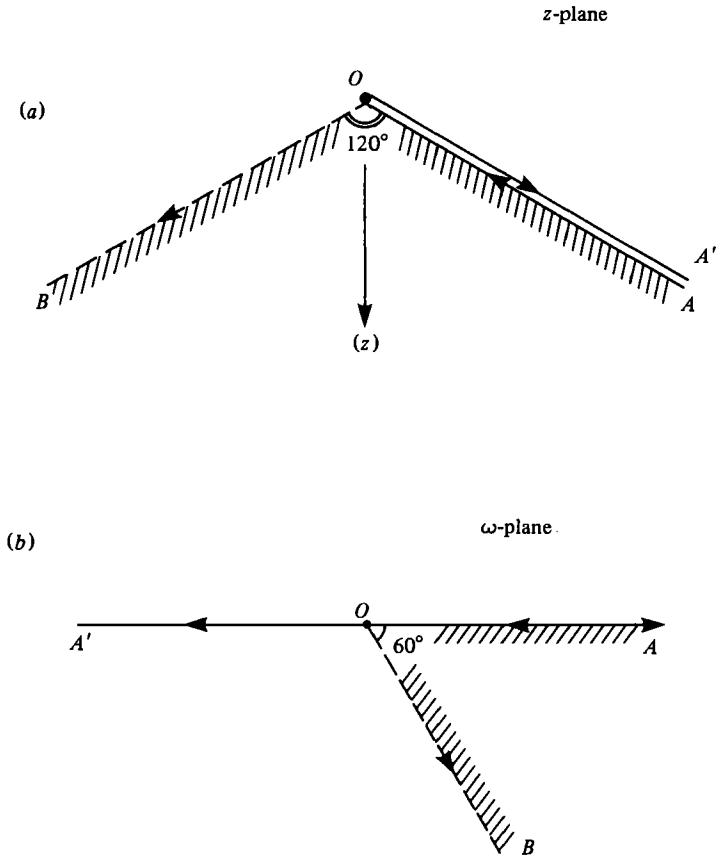

FIGURE 3. Parametric representation of the Stokes corner flow (*a*) in the z-plane, (*b*) in the ω-plane.

Hence (5.1) is satisfied if

$$r = \frac{\sqrt{3}}{\omega - t}, \tag{6.4}$$

which is real when ω is real. Moreover

$$z_t^*(\omega) = -\tfrac{1}{2}g\, e^{-i\pi/3}(\omega - t), \tag{6.5}$$

so from (4.3)

$$\chi_\omega = -\tfrac{1}{4}g^2(\omega - t)^2. \tag{6.6}$$

Integration with respect to ω gives

$$\chi = -\tfrac{1}{12}g^2(\omega - t)^3 = \tfrac{2}{3}ig^{\frac{1}{2}}z^{\frac{3}{2}}, \tag{6.7}$$

the well-known expression for the velocity potential in a Stokes corner flow.

Paradoxically, when $t > \omega$ the particles in the free surface, according to (6.1), reverse their direction and slide again down the *forward* face of the wave, instead of down the rear face as might be expected. The paradox is resolved by considering the situation in the ω-plane (figure 3*b*). There it is seen that the forward face of the wave (OA in figure 3*a*) corresponds to the positive real axis of $\omega - t$, but the rear face OB corresponds to the line $\arg(\omega - t) = -\frac{1}{3}\pi$. The point $\omega - t = 0$ is a branch point of z, and when $\omega - t < 0$ the particles go onto another sheet of the Riemann surface.

All the particles in the interior of the fluid correspond to $\mathscr{I}(\omega) < 0$), and since ω is not real the representation there is *not* Lagrangian. Thus the particles do not have to follow a path on which ω is constant.

It remains to verify that the two boundary conditions (3.4) are in fact satisfied on OB. This would follow from the symmetry of the expression (6.9) for χ, but from (6.1) it is less obvious. However, direct substitution into (4.8) gives us

$$2p = \tfrac{1}{4}g^2(\omega-\omega^*)\,[(\omega-t)\,e^{i\pi/3}-(\omega^*-t)\,e^{-i\pi/3}], \tag{6.8}$$

which vanishes both when $\omega = \omega^*$ (that is on OA, OA'), and when

$$(\omega-t)\,e^{i\pi/3} = (\omega^*-t)\,e^{-i\pi/3} \tag{6.9}$$

(that is on OB).

Clearly if $z(\omega, t)$ is a polynomial in ω, then the expression for $p(\omega, \omega^*, t)$ will, by (4.8), be a polynomial in ω and ω^*, with a factor $\omega-\omega^*$, so we can write in general

$$\frac{8p}{g^2} = (\omega-\omega^*)\,G(\omega, \omega^*, t), \tag{6.10}$$

and the free surface, apart from $\omega = \omega^*$, will be given by $G = 0$. To show that the second condition $Dp/Dt = 0$ is satisfied on this surface, it is sufficient to show that $DG/Dt = 0$ when $G = 0$.

In the present case

$$G \equiv (\omega-t)\,e^{i\pi/3}-(\omega^*-t)\,e^{-i\pi/3}, \tag{6.11}$$

and a direct calculation using (4.9) with $F = G$ gives

$$z_\omega z^*_{\omega^*}\frac{DG}{Dt} = -\tfrac{1}{4}g^2[(\omega-t)^2\,e^{2i\pi/3}-(\omega-t)^2\,e^{-2i\pi/3}]. \tag{6.12}$$

Since G is a factor of the right-hand side of (6.12), it follows that DG/Dt vanishes on OB as required.

We remark that, if $z^{(1)}$ denotes the steady flow (6.1), then

$$z^{(2)} = z^{(1)}-\tfrac{1}{2}gt^2 \tag{6.13}$$

represents a gravity-free flow satisfying the homogeneous boundary condition

$$z_{tt} = irz_\omega \tag{6.14}$$

with r given by (6.4). Moreover

$$z^{(2)} = \tfrac{1}{4}g\,e^{i\pi/3}S, \tag{6.15}$$

where

$$\begin{aligned} S &= (\omega-t)^2-2\,e^{-i\pi/3}t^2 \\ &= \omega^2-2\omega t+\sqrt{3}\,it^2 \\ &= t^2[(\omega/t)^2-2(\omega/t)+\sqrt{3}\,i]. \end{aligned} \tag{6.16}$$

Thus $z^{(2)}$ represents a self-similar flow, expanding with time proportionally to t^2.

Higher-order polynomial expressions also exist satisfying (6.16) with the same function as in (6.4). For example, the cubic

$$z = \omega^3-\tfrac{3}{2}(1+\tfrac{1}{2}\sqrt{3}\,i)\,t\omega^2+\tfrac{3}{2}\sqrt{3}\,it^2\omega+\tfrac{3}{4}t^3, \tag{6.17}$$

for which the contours $p = 0$ are shown in figure 4. One branch, other than the real axis of ω, passes through the point $\omega/t = 1$. The branch points, given by the vanishing

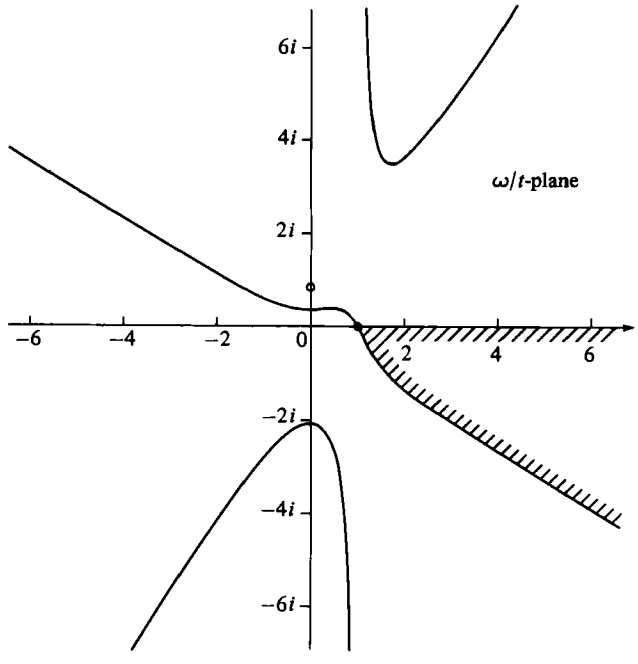

FIGURE 4. Loci of $p = 0$ corresponding to the flow given by equation (7.8) in the ω-plane.

of z_ω, are at $\omega/t = 1$ and $\frac{1}{2}\sqrt{3}\,i$. Hence a possible domain of flow would appear to be the shaded area shown in figure 4. However, on further investigation it appears that the second boundary condition $Dp/Dt = 0$ is not satisfied on any of the contours $p = 0$ other than the real axis. Hence (6.17), and similar expressions of higher order, do not represent complete solutions.

7. The 45° rotor

An interesting exact solution of the homogeneous equation (5.2) is the expression

$$z = \omega e^{-(1+i)t+i\epsilon}, \tag{7.1}$$

where ϵ is a constant phase, to be determined. We have clearly

$$z_{tt} = 2i\omega z_\omega, \tag{7.2}$$

so that z satisfies (5.2) with $r = 2\omega$. Moreover from (4.3)

$$\chi_\omega = -(1-i)\,\omega e^{-2t}, \tag{7.3}$$

hence

$$\chi = \frac{e^{3i\pi/4}\omega^2 e^{-2t}}{\sqrt{2}}. \tag{7.4}$$

Choosing $\epsilon = \frac{3}{8}\pi$, we may write

$$\chi = \frac{e^{2it}}{\sqrt{2}} z^2, \tag{7.5}$$

which identifies the flow with the 45° 'rotating hyperbola' discovered in paper II. The flow is sketched in figure 5(*a*).

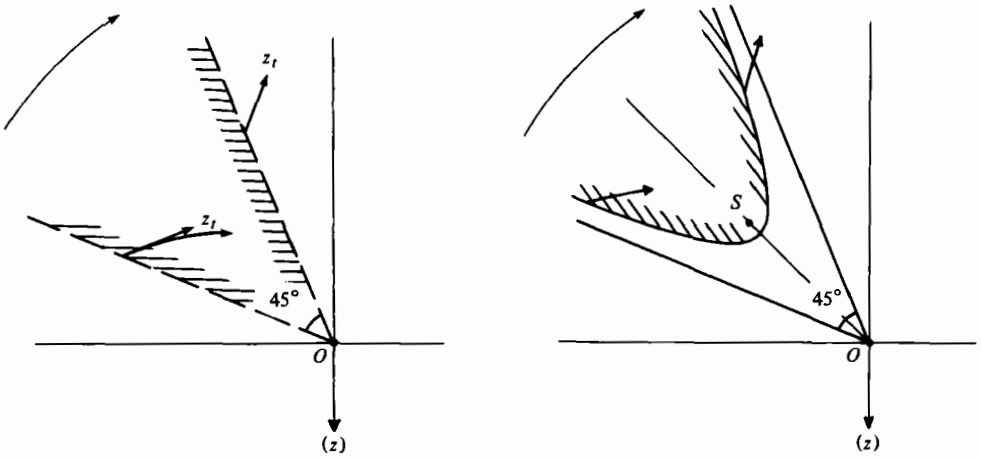

(a) (b)

FIGURE 5. The 45° rotating corner flow: (a) equation (7.1); (b) equation (7.10). In each case the flow is extended by reflection in the origin O.

Direct calculation using (4.8) gives for the pressure field

$$-2p = (\omega-\omega^*)[(1+i)\omega-(1-i)\omega^*]e^{-2t}. \tag{7.6}$$

So, apart from the real axis $\omega = \omega^*$ there is a second free surface $p = 0$ given by $\arg\omega = -\frac{1}{4}\pi$. Setting

$$G \equiv [(1+i)\omega-(1-i)\omega^*]e^{-2t}, \tag{7.7}$$

we find also from (4.9) that

$$\frac{DG}{Dt} = -2G. \tag{7.8}$$

Hence the second boundary condition is also satisfied on $G = 0$.

We see from (7.1) that

$$W^* = z_t(\omega^*) = -(1+i)\omega^* e^{-(1+i)t+i\epsilon}. \tag{7.9}$$

For points on the trailing face of the wedge ($\omega = \omega^*$) we have $z_t = -(1+i)z$. Hence the particles spiral inwards towards the centre along 45° spirals.

For points on the other face, $\arg\omega = -\frac{1}{4}\pi$, we have $\omega^*/\omega = i$, hence $z_t = (1-i)z$ and the particles spiral outwards.

The single-term expression (7.1) represents only the special case of the '45° rotor' when the boundary has a sharp corner. By adding to (7.1) a second term, so that

$$z = \omega e^{-(1+i)t+3i\pi/8} + \omega^{-1} e^{(1-i)t+i\pi/8} \tag{7.10}$$

we obtain a more general flow in which the free surface is a 45° hyperbola, with rounded vertex, rotating about its centre $z = 0$ (see figure 5b). The potential $\chi(\omega, t)$ satisfies

$$\chi = \frac{e^{2it}}{\sqrt{2}}z^2 - \sqrt{2}\,i \tag{7.11}$$

and the equation of the free surface is

$$\tfrac{1}{2}i e^{2it}z^2 + \text{c.c.} + \sqrt{\tfrac{1}{2}}zz^* = -1, \tag{7.12}$$

a special case of paper II, equation (4.1). In the present formulation $z(\omega, t)$ has a branch point ($z_\omega = 0$) when

$$\omega = e^{t-i\pi/8}, \quad z = 2e^{-it+i\pi/4}, \tag{7.13}$$

which lies at a focus of the hyperbola, that is in the interior of the flow. But this is also a branch point of the velocity $z_t(\omega^*)$, so that altogether the flow is non-singular.

The flow just described is itself a highly special case of the class of hyperbolic flows, with variable angle between the asymptotes, suggested in II as representing the tip of a plunging breaker. However, their parametric representation would in general seem to involve transcendental functions of t.

8. Upwelling flows

We now discuss a different, and in some ways simpler, class of flows than the two types just described. These may be called 'upwelling flows' for reasons that will become apparent.

We first choose a very simple form of (5.1). In fact let us take $r = -2/t$, independent of ω, and to save writing set

$$i\omega = \varpi \tag{8.1}$$

so that the non-homogeneous boundary condition (5.1) becomes

$$\tfrac{1}{2}t(z_{tt} - g) = z_\varpi. \tag{8.2}$$

This must be satisfied when ϖ is *pure imaginary*, that is when $\varpi + \varpi^* = 0$.

Clearly (8.2) is satisfied by the expression

$$z = -\tfrac{1}{2}gt\varpi. \tag{8.3}$$

Moreover

$$z_\varpi = -\tfrac{1}{2}gt, \tag{8.4}$$

$$W = z_t^*(-\varpi) = \tfrac{1}{2}g\varpi, \tag{8.5}$$

so from (4.6)

$$\chi_\varpi = -\tfrac{1}{4}g^2t\varpi, \tag{8.6}$$

giving

$$\chi = -\tfrac{1}{8}g^2t\varpi^2 = -\frac{z^2}{2t}. \tag{8.7}$$

This flow is shown in figure 6. The free surface $\mathscr{R}(\varpi) = 0$ is the y-axis, $x = 0$. The velocity potential is

$$\phi = -\frac{x^2 - y^2}{2t} \tag{8.8}$$

and the streamlines are

$$\psi = -\frac{xy}{t} = \text{constant}, \tag{8.9}$$

which are rectangular hyperbolae. For $t > 0$ the flow represents a decelerated upwelling, in which the vertical and horizontal components of flow are given by

$$\phi_x = -\frac{x}{t}, \quad \phi_y = \frac{y}{t} \tag{8.10}$$

respectively, the axis of x being vertically downwards.

To verify that horizontal surface $x = 0$ is indeed a surface of constant pressure, note that the horizontal pressure gradient is in general given by

$$-p_y = v_t + (uv_x + vv_y), \tag{8.11}$$

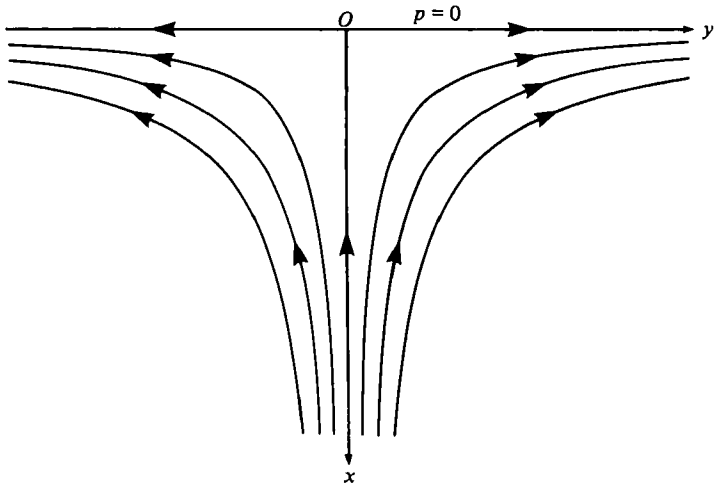

FIGURE 6. Streamlines of the upwelling flow (8.7).

where $(u, v) = (\phi_x, \phi_y)$. From (8.10) the terms on the right of (8.11) are equal to $-y/t^2$, 0 and y/t^2 respectively. Hence $p_y = 0$ everywhere. Alternatively we may remark that in the Bernoulli equation

$$-p = \phi_t + \tfrac{1}{2}(\phi_x^2 + \phi_y^2) - gx \tag{8.12}$$

the acceleration term ϕ_t is exactly balanced by the usual pressure defect $-\frac{1}{2}(\nabla\phi)^2$.

For $t < 0$, ϕ_x becomes positive (when $x > 0$), and instead of a decelerated upwelling we have an accelerated downwelling.

9. Complementary upwelling flows

We now seek flows complementary to the upwelling flow described in § 8. That is to say, we seek solutions to the homogeneous boundary condition

$$\tfrac{1}{2}tz_{tt} = z_w \tag{9.1}$$

to be satisfied when $w + w^* = 0$.

Let us try the polynomial expression

$$z = b_n w^n + b_{n-1} w^{n-1} + \ldots + b_0, \tag{9.2}$$

the coefficients b_n being functions of the time t only. Substituting into (9.1), we obtain

$$\left.\begin{aligned} \tfrac{1}{2}t\ddot{b}_n &= 0, \\ \tfrac{1}{2}t\ddot{b}_{n-1} &= nb_n, \\ \tfrac{1}{2}t\ddot{b}_{n-2} &= (n-1)b_{n-1}, \\ &\vdots \qquad\quad \vdots \\ \tfrac{1}{2}t\ddot{b}_0 &= b_1. \end{aligned}\right\} \tag{9.3}$$

Clearly b_n must be of the form $At + B$, with A and B constant. Since the equations (9.3) are linear, the simplest solutions of (9.2) can be separated into two fundamental

classes, those in which $A = 1, B = 0$, and those in which $A = 0, B = 1$. Denoting these by P_n and Q_n respectively, we find by straightforward integration, as far as $n = 3$,

$$\left.\begin{aligned} P_0 &= t, \\ P_1 &= t\varpi + t^2, \\ P_2 &= t\varpi^2 + 2t^2\varpi + \tfrac{2}{3}t^3, \\ P_3 &= t\varpi^3 + 3t^2\varpi^2 + 2t^3\varpi + \tfrac{1}{3}t^4, \end{aligned}\right\} \tag{9.4}$$

and

$$\left.\begin{aligned} Q_0 &= 1, \\ Q_1 &= \varpi + 2t\ln|t|, \\ Q_2 &= \varpi^2 + 4t\varpi\ln|t| + 4t^2(\ln|t| - \tfrac{3}{2}), \\ Q_3 &= \varpi^3 + 6t\varpi^2\ln|t| + 12t^2\varpi(\ln|t| - \tfrac{3}{2}) + 4t^3(\ln|t| - \tfrac{7}{3}). \end{aligned}\right\} \tag{9.5}$$

The complete polynomial solution will be of the form

$$z = \sum_n (A_n P_n + B_n Q_n). \tag{9.6}$$

Each of the flows P_n is self-similar, as can be seen by writing it in the form

$$P_n(\varpi, t) = t^{n+1} P_n(\varpi/t, 1). \tag{9.7}$$

In fact these flows are limiting cases of the self-similar flows described in § 9 of Longuet-Higgins (1976), in the limit as $\lambda \to 1$.

On the other hand, the flows represented by Q_n are not self-similar, nor is any combination of the P_n and Q_n involving two or more non-zero coefficients A_n or B_n.

10. Discussion: linear flows

To interpret the solutions physically, we note first that all expressions linear in ϖ must correspond to a free-surface profile that is a straight line. Similarly, any expression that is quadratic in ϖ has a surface profile that is a parabola, whose orientation and dimensions may vary in time. Every solution of the third degree in ϖ corresponds to a parametric cubic, and so on.

As an example consider the linear flow P_1. We have then

$$z = t\varpi + t^2, \tag{10.1}$$

so

$$z_\varpi = t, \quad z_t = \varpi + 2t. \tag{10.2}$$

To find the velocity potential χ we note that on the free surface $\varpi^* = -\varpi$, so the general boundary condition

$$\chi_\varpi = z_t^*(-\varpi)\, z_\varpi(\varpi) \tag{10.3}$$

gives

$$\chi_\varpi = -t\varpi + 2t^2, \tag{10.4}$$

hence

$$\chi = -\tfrac{1}{2}t\varpi^2 + 2t\varpi \tag{10.5}$$

to within a function of the time t. The pressure p is now found from the equivalent of (4.8), namely

$$-2p = (\chi_t + \chi_t^*) + z_t^*(-\varpi)\, z_t(-\varpi^*) - 2f - [z_t(\varpi)\, z_t^*(-\varpi) + z_t^*(\varpi^*)\, z_t(-\varpi^*)]. \tag{10.6}$$

With suitable choice of f this gives

$$-2p = (\varpi+\varpi^*)[\tfrac{1}{2}(\varpi+\varpi^*)+2t]. \tag{10.7}$$

The locus of $p = 0$ is therefore

$$\varpi+\varpi^* = 0, \quad z+z^* = 2t^2, \tag{10.8}$$

together with the parallel line

$$\varpi+\varpi^* = -4t, \quad z+z^* = -2t^2. \tag{10.9}$$

To calculate Dp/Dt we use the general formula analogous to (4.9), namely

$$\frac{DF}{Dt} = F_t + K'F_w + K'^*F_{w^*}, \tag{10.10}$$

where $F = -2p$ and

$$K' = [z_t(-\varpi^*) - z_t(\varpi)]/z_\varpi. \tag{10.11}$$

Hence

$$\frac{Dp}{Dt} = (\varpi+\varpi^*)[(\varpi+\varpi^*)/t+1]. \tag{10.12}$$

This vanishes on the free surface (10.8) but not on the parallel surface (10.9). In other words, (10.9) represents a surface that is *not* moving with the fluid particles.

Clearly the non-homogeneous flow (8.3) is a special case of the flow P_1 when seen in an accelerated frame of reference.

11. Quadratic flows

The second-order flows ($n = 2$) are the simplest to have a branch point ($z_\varpi = 0$) in the finite part of the plane. This occurs always at the focus of the parabola. Thus for P_2 we have

$$z_\varpi = 2t\varpi + 2t^2, \tag{11.1}$$

which vanishes when $\varpi = -t$, $z = -\frac{1}{3}t^3$. The particle velocity W^* is given by

$$W = z_t^*(-\varpi) = \varpi^2 - 4t\varpi + 2t^2, \tag{11.2}$$

and since $W_\varpi = 2\varpi - 4t$, which does not vanish at the branch point, this is a genuine singularity. The flow must therefore be taken in some domain excluding the focus, i.e. outside the parabola.

The corresponding velocity potential is found to be

$$\chi = \tfrac{1}{2}t\varpi^4 - 2t^2\varpi^3 - 2t^3\varpi^2 + 4t^4\varpi^3, \tag{11.3}$$

and the pressure field is given by

$$2p = (\varpi+\varpi^*)[\tfrac{1}{2}(\varpi-\varpi^*)(\varpi^2-\varpi^{*2}) + 4t(\varpi^2+\varpi^{*2}) - 8t^2(\varpi+\varpi^*) - 8t^3]. \tag{11.4}$$

The loci of $p = 0$ in the planes of ω and z are shown in figure 7. On the branches of the locus other than $\varpi+\varpi^* = 0$ it is found that Dp/Dt does not vanish, nor is it a function of t only, so these do not correspond to free surfaces.

Similar remarks apply to the flow $z = Q_2$.

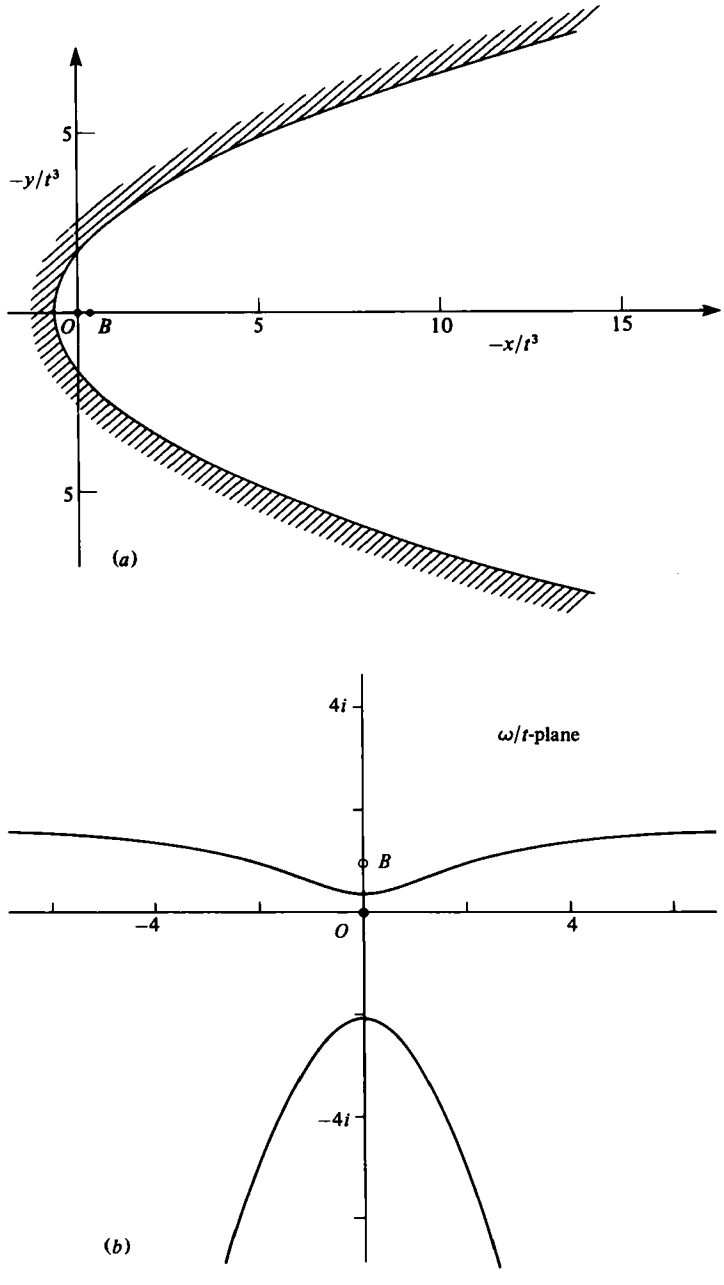

FIGURE 7. The quadratic flow $z = P_2$. (*a*) Free surface in the z-plane; (*b*) contours of $p = 0$ in the ω-plane.

12. Cubic flows

The case $n = 3$ is of special interest as being the simplest case for which the free surface can intersect itself.

Consider the flow P_3. We have

$$z = t\varpi^3 + 3t^2\varpi^2 + 2t^3\varpi + \tfrac{1}{3}t^4. \tag{12.1}$$

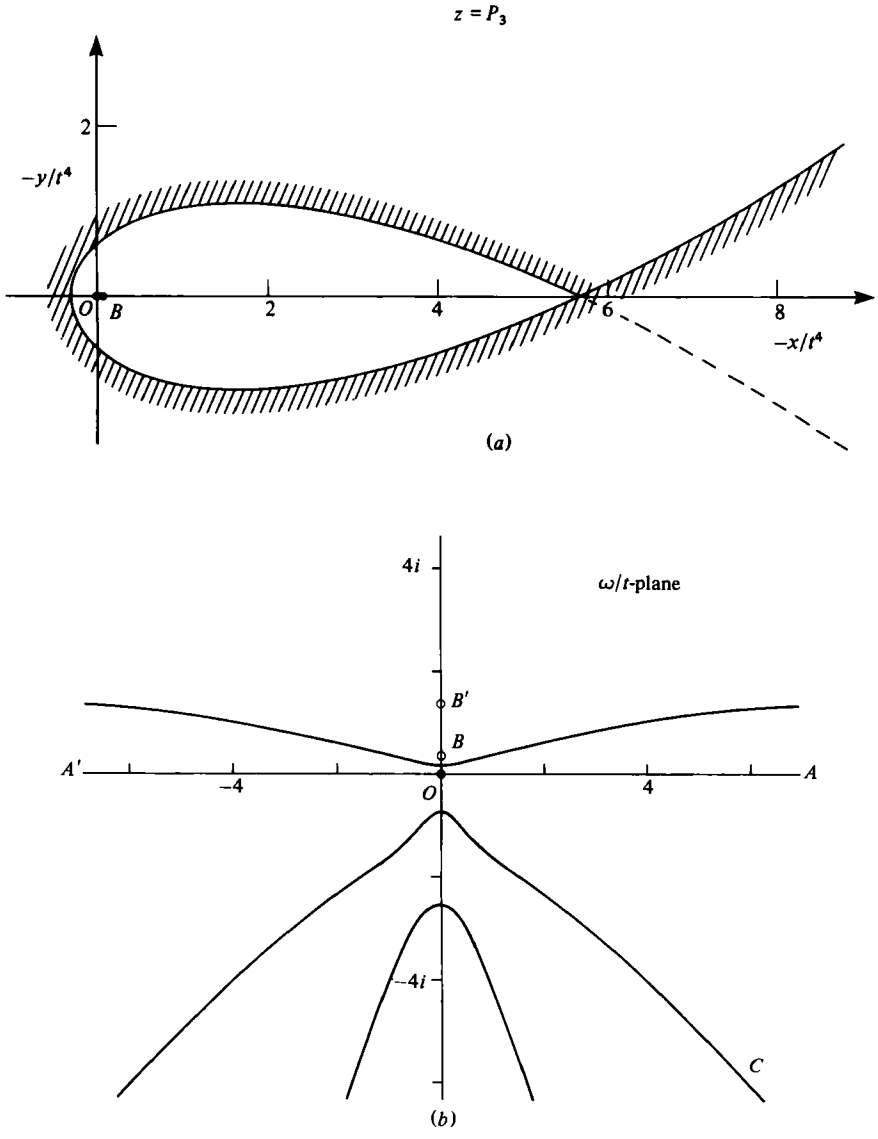

FIGURE 8. The cubic upwelling $z = P_3$. (*a*) Free surface in the z-plane; (*b*) contours of $p = 0$ and branch points in the ω-plane.

At the free surface, ϖ being imaginary, we may write $\varpi/t = i\mu$, μ real, so on separating real and imaginary parts in (12.1),

$$\left.\begin{aligned} x/t^4 &= -3\mu^2 + \tfrac{1}{3}, \\ y/t^4 &= -\mu^3 + 2\mu. \end{aligned}\right\} \tag{12.2}$$

The profile is shown in figure 8(*a*). It intersects the x-axis when $\mu = 0$ and $\pm\sqrt{2}$, that is in the points $z/t^4 = \frac{1}{3}$ and $-\frac{17}{3}$ respectively, the latter being a double point on the curve. Stationary values of y occur when $\mu^2 = \frac{2}{3}$ and $z/t^4 = -\frac{5}{3} \pm \sqrt{\frac{32}{27}}\, i$. The

'aspect ratio' of the loop, that is to say the width of the loop at its widest section divided by the distance between the vertex and the node, is

$$\tfrac{4}{9}\sqrt{\tfrac{2}{3}} = 0{\cdot}3629. \tag{12.3}$$

The maximum width is one-third of the way from the vertex to the node.

The branch points of z are given by the vanishing of

$$z_w = 3tw^2 + 6t^2w + 2t^3, \tag{12.4}$$

that is

$$w/t = -1 \pm \sqrt{\tfrac{1}{3}} \tag{12.5}$$

so

$$z/t^4 = \tfrac{1}{3}(1 \pm 2\sqrt{\tfrac{1}{3}}). \tag{12.6}$$

These are marked B and B' in figure 8(a). In figure 8(b) B lies very close to the origin and B' is not shown because it lies on another sheet of the Riemann surface.

The velocity potential corresponding to (12.1) is found to be

$$\chi = -\tfrac{1}{2}tw^6 + \tfrac{12}{5}t^2w^5 + 4t^3w^4 - \tfrac{20}{3}t^4w^3 - 2t^5w^2 + \tfrac{8}{3}t^6w, \tag{12.7}$$

and the pressure is given by

$$\begin{aligned} 2p = [&-\tfrac{1}{2}(w^6 + w^3w^{*3}) - \tfrac{6}{5}t(4w^5 - 5w^3w^{*2}) + 6t^2(2w^4 - w^3w^* - 3w^2w^{*2}) \\ &+ 4t^3(7w^3 + 9w^2w^*) - 18t^4(w^2 + ww^*) - 8t^5w] + \text{c.c.} \end{aligned} \tag{12.8}$$

13. Comparison with observation

In figure 9 we compare the observed surface profile of figure 1 with the curve of equation (12.2). The agreement with the forward face of the wave is remarkable.

A second comparison can be made with the recent numerical calculations of breaking waves by Vinje & Brevig (1981), shown in figure 10. Inserted in the figure are straight lines, each representing the axis of symmetry of a cubic curve fitted to the lower part of the profile. Table 1 shows the lengths of the corresponding axes; $2a$ is the distance between the two points where the curve intersects the axis, and $2b$ is twice the maximum distance of the lower part of the profile from the axis. The 'aspect ratios' b/a are given in the third column of table 1, and will be seen to be close to the theoretical ratio (12.3).

In figure 10 the orientation of the axes is nearly constant; the angle of inclination of the horizontal varies only between about 37° and 47°. The length $2b$ of the minor axis is shown as a function of the time in figure 11. The plotted points have been fitted with a curve of the form $C(t-t_0)^4$, where $t_0 > 0$. If this were followed precisely it would indicate that the dimensions of the 'tube' tended to zero as $t \to t_0$.

The curve of figure 8 may indeed be typical of plunging breakers. It was remarked by New (1981) that profiles were very often fitted quite accurately by an *ellipse* with axes in the ratio $\sqrt{3}:1$. In figure 12 we show a comparison between the cubic curve of figure 8(a) and a '$\sqrt{3}$-ellipse' having the same minimum radius of curvature. Again the agreement is close.

The only part of the free surface described so far is the forward face of the wave. However, the complete locus $p = 0$ (see (12.8)) contains another branch within the fluid, labelled II in figure 13(a). On this branch the second boundary condition $Dp/Dt = 0$ is not generally satisfied (as it is on I). Moreover the curve is symmetric

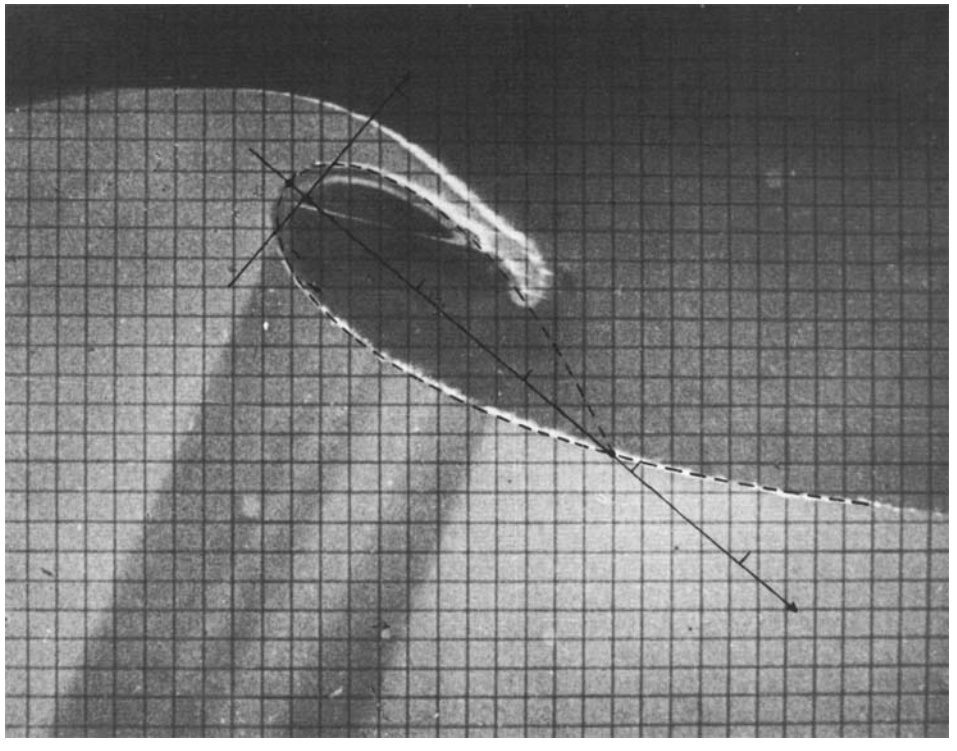

FIGURE 9. Comparison of $z = A_3 P_3$ with the observed profile in figure 1.

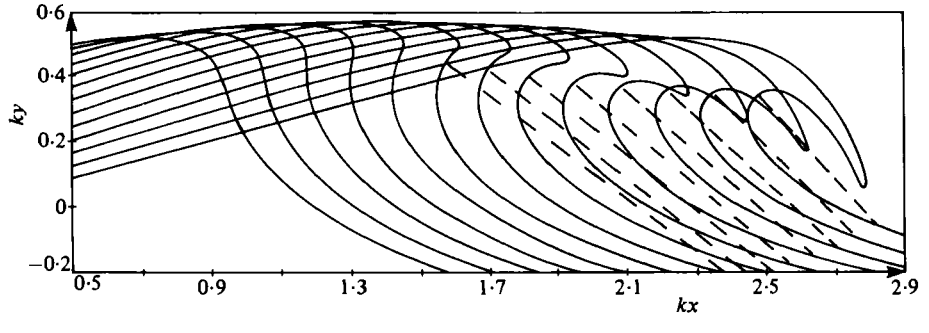

FIGURE 10. Successive profiles of a wave breaking in deep water (after Vinje & Brevig 1981, figure 4.12).

about the real axis of z. Nevertheless, since the pressure p has a stationary point (saddle point) on the real axis between I and II, it appears that only a slight asymmetric perturbation of the flow would be sufficient to alter the free surface to the form III, corresponding very nearly to the surface of a plunging breaker. Near the tip of the jet, the perturbed flow may locally take the form described in paper II.

Figure 13 (*b*) shows the same flow $z = P_3$ but at a different time $t = 0{\cdot}5$. Apart from the perturbation, which is seen to be a small part of the total flow, the surfaces in figures 13 (*a*) and 13 (*b*) are precisely similar.

t	$2a$ (mm)	$2b$ (mm)	b/a	θ
6	64·0	26·0	0·41	37°
7	55·5	21·0	0·38	38°
8	52·0	19·0	0·37	39°
9	41·5	15·0	0·36	40°
10	40·5	14·0	0·35	41°
11	36·5	12·5	0·34	43°
12	32·5	11·2	0·35	45°
13	29·5	10·5	0·36	47°

TABLE 1. Measured parameters of deep-water wave crests, from Vinje & Brevig (1981, figure 4.12)

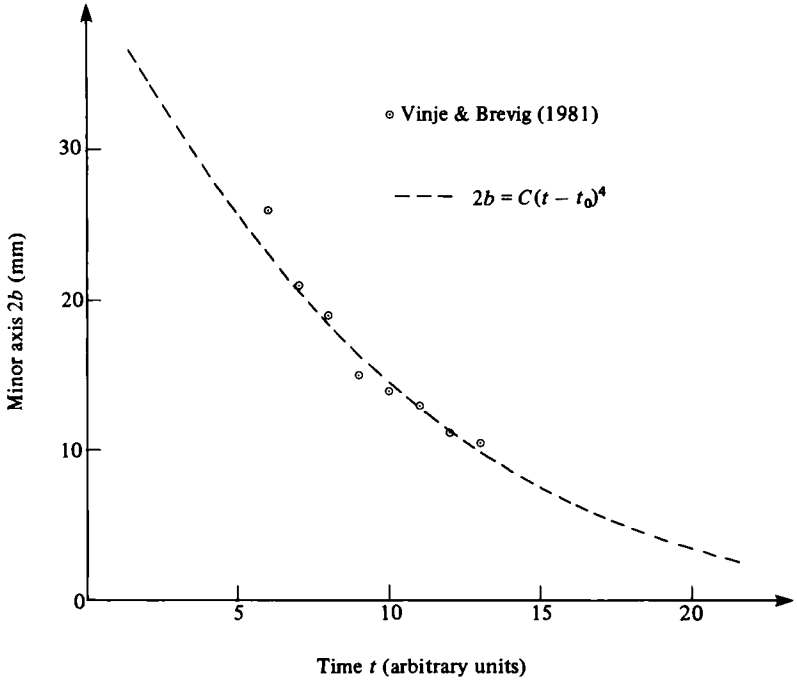

FIGURE 11. Time variation of the length of the minor axis in figure 10.

In the expression for the pressure p the terms of highest order in ω are given by

$$2p = \tfrac{1}{2}(\omega^2 - \omega^{*3})^2 + O(\varpi^5) \tag{13.1}$$

so that one of the asymptotes is $\arg\omega = -\frac{1}{3}\pi$, corresponding to a surface inclined asymptotically at 120° to the forward face of the wave.

The second solutions Q_n will not be discussed in detail, except to remark that Q_3 has one branch point on either side of the free surface $\omega = \omega^*$ whenever $\ln|t| < \frac{3}{2}$. Thus $z = Q_3$, unlike $z = P_3$, is not a physically possible flow. However, it may be worth noting that over limited intervals of time the expression

$$z = P_3 + i\eta Q_3 \tag{13.2}$$

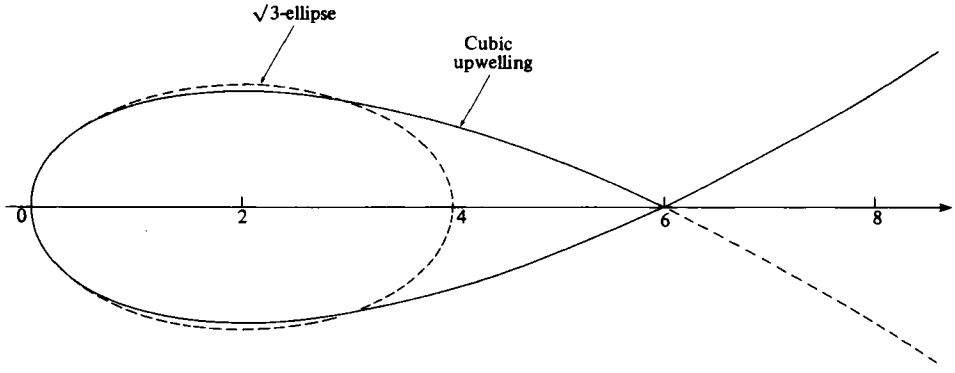

FIGURE 12. Comparison of the cubic curve $z = P_3$ given by (12.2) and an ellipse having axes in the ratio $\sqrt{3}:1$.

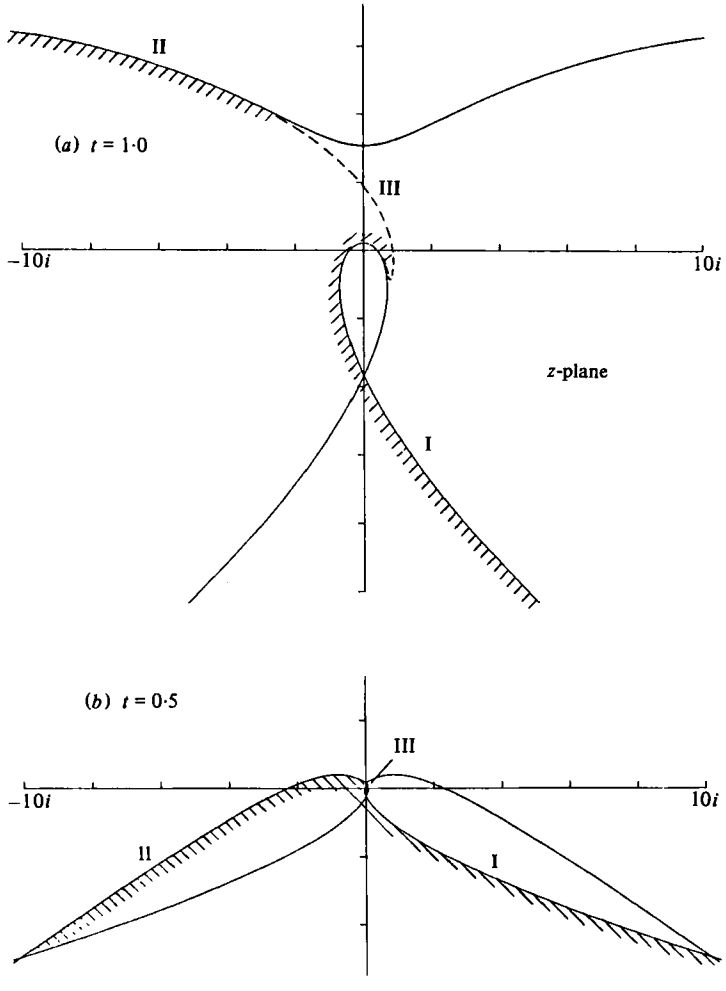

FIGURE 13. Contours of the pressure for $z = P_3$ in the physical plane: (*a*) when $t = 1$; (*b*) when $t = 0{\cdot}5$.

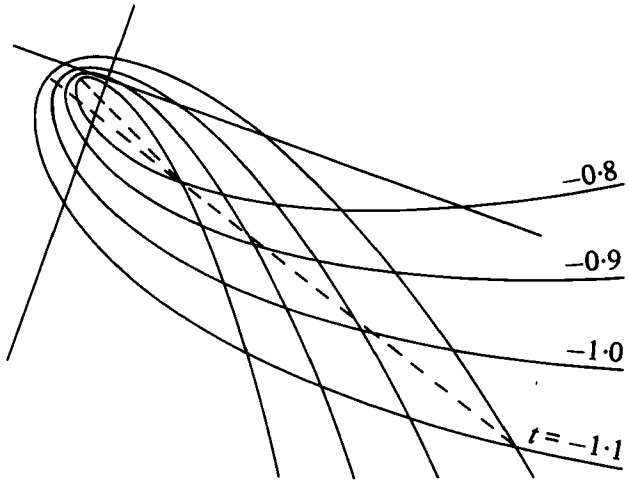

FIGURE 14. Successive profiles of the free surface for the flow $z = P_3 + 0{\cdot}1iQ_3$.

where η is a real, positive constant, $\ll 1$, represents a flow in which the asymptotes rotate clockwise, as does the nodal loop (see figure 14). This agrees qualitatively with the numerical profiles shown in figure 10.

14. Conclusion

We have shown how a parametric description of the fluid flow, involving only elementary functions of the parameter ω, can describe some outstanding features of an overturning gravity wave, particularly the asymptotic form of the front face of the wave. We have confirmed the suggestion in III that the analytic description probably involves a branch point. We have also described the flow near the tip of the 'jet', in a special case.

A complete solution should ideally give an account of the whole development of the flow, including the rear face of the wave. There is reason to believe that this may be possible by combining or perturbing the solutions given in the present paper.

REFERENCES

JOHN, F. 1953 Two-dimensional potential flows with a free boundary. *Communs Pure Appl. Math.* **6**, 497–503.

LONGUET-HIGGINS, M. S. 1976 Self-similar, time-dependent flows with a free surface. *J. Fluid Mech.* **73**, 603–620.

LONGUET-HIGGINS, M. S. 1980*a* (Paper I) A technique for time-dependent, free-surface flows. *Proc. R. Soc. Lond.* A **371**, 441–451.

LONGUET-HIGGINS, M. S. 1980*b* (Paper II) On the forming of sharp corners at a free surface. *Proc. R. Soc. Lond.* A **371**, 453–478.

LONGUET-HIGGINS, M. S. 1981 (Paper III) On the overturning of gravity waves. *Proc. R. Soc. Lond.* A **376**, 377–400.

MILLER, R. L. 1957 Role of vortices in surf zone prediction, sedimentation and wave forces. In *Beach and Nearshore Sedimentation* (ed. R. A. Davis & R. L. Ethington), pp. 92–114. Tulsa, Oklahoma: Soc. of Economic Palaeontologists and Mineralogists.

NEW, A. L. 1981 Breaking waves in water of finite depth. *British Theor. Mech. Colloq., Bradford,* 6–9 *April* 1981 (abstract only).

STOKES, G. G. 1880 On the theory of oscillatory waves. Appendix B: Considerations relative to the greatest height of oscillatory waves which can be propagated without change of form. *Mathematical Physical Papers*, vol. I, pp. 225–228. Cambridge University Press.

VINJE, T. & BREVIG, P. 1981 Breaking waves on finite water depths: a numerical study. *Ship Res. Inst. of Norway, Rep.* R-111.81.